

RESEARCH

Open Access



MiR-451a attenuates hepatic steatosis and hepatitis C virus replication by targeting glycerol kinase

Swagata Majumdar¹, Deeya Roy Chowdhury¹, Bidhan Chandra Chakraborty², Abhijit Chowdhury³, Simanti Datta^{1,2} and Soma Banerjee^{1*} 

Abstract

Background Lipotoxicity is one of the causes for the progression of fatty liver in chronic hepatitis (CH) towards end-stage liver diseases. The role of miRNAs in the signalling pathways of lipid metabolism has been studied, but their direct targets in this pathway have not been identified yet. Here, we have characterized a downregulated miRNA in CH namely miR-451a, which has a direct impact on the lipid metabolism pathway.

Methods Liver tissue samples and blood were collected from CHC/CHB patients and normal individuals. Huh7 and SNU449 cell lines were used for in vitro assays. Expressions of miRNA/mRNAs and proteins were confirmed by qRT-PCR and immuno-blot analysis. Oil Red O staining, Colorimetric, and Fluorometric assay kit were used to quantify triglyceride (TG) and cholesterol from tissue and serum, respectively. Target prediction and pathway analysis were performed using Targetscan, miRWalk, and DAVID respectively. 3'UTR-Luciferase assay and Co-immuno-precipitation were conducted to determine direct interaction between miRNA-mRNA and protein-protein, respectively. Unpaired two-tailed Student's t-test and Mann-Whitney test were employed as required using GraphPad prism. $P < 0.05$ was considered as significant.

Results The miRNA, miR-451a was selected as one of the downregulated miRNAs in progressive liver disease stages of CHC and CHB. Target identification and pathway analysis of this miRNA revealed that lipid metabolism pathway gene, glycerol kinase (GK), could be the target of this miRNA. Subsequent 3'UTR Luciferase assay and immuno-blot analysis confirmed the binding of miR-451a to GK. Though both hepatitis viruses, HCV and HBV, could alter the lipid metabolism pathways, intracellular TG and cholesterol content were observed to be significantly higher upon HCV infection only. It also suppressed the expression of miR-451a, resulting in overshooting of GK expression. GK interacted positively with the transcription factor SREBP1, which led to overexpression of Fatty acid synthase, Acetyl-CoA Carboxylase, and Stearoyl-CoA desaturase. As a result, intracellular fatty acids, TG, and cholesterol synthesis and accumulation heightened but trafficking dropped, resulting in hypo-cholesterolemia in blood. While, restoration of miR-451a impeded lipid accumulation, reduced steatohepatitis and suppressed HCV replication as well.

*Correspondence:
Soma Banerjee
somabanerjee70@gmail.com

Full list of author information is available at the end of the article



© The Author(s) 2025. **Open Access** This article is licensed under a Creative Commons Attribution-NonCommercial-NoDerivatives 4.0 International License, which permits any non-commercial use, sharing, distribution and reproduction in any medium or format, as long as you give appropriate credit to the original author(s) and the source, provide a link to the Creative Commons licence, and indicate if you modified the licensed material. You do not have permission under this licence to share adapted material derived from this article or parts of it. The images or other third party material in this article are included in the article's Creative Commons licence, unless indicated otherwise in a credit line to the material. If material is not included in the article's Creative Commons licence and your intended use is not permitted by statutory regulation or exceeds the permitted use, you will need to obtain permission directly from the copyright holder. To view a copy of this licence, visit <http://creativecommons.org/licenses/by-nc-nd/4.0/>.

Conclusion These findings suggest that the alteration in the hepatic lipid profile upon HCV/HBV infection is attributed to the downregulation of miR-451a, which has the potential to restrict the expression of GK and SREBP1 in the TG biosynthesis pathway, implying that supplementation of miR-451a may be a potential therapeutic strategy for impeding CHC.

Keywords miR-451a, Hepatitis C virus, Lipid metabolism, Hepatic steatosis

Introduction

Chronic hepatitis C and B virus (HCV and HBV) infections remain one of the major global health burdens, leading to liver cirrhosis (LC), liver failure, and hepatocellular carcinoma (HCC) [1, 2]. Despite the availability of preventive vaccines for HBV and direct acting antivirals (DAA) for both HBV and HCV, each day about 3,500 patients die from liver diseases caused by these viruses worldwide [3]. Hence, an in-depth understanding of the molecular mechanism of viral hepatitis and its progression towards endstage liver diseases such as LC and HCC needs to be explored further. Host-virus interactions play a pivotal role in successful viral replication and persistence [4, 5]. Hence, identification of those pathways is necessary for the selection of therapy and the discovery of novel therapeutics.

The liver is the major organ for lipid metabolism including fatty acid (FA) intake, lipid biosynthesis, FA oxidation and lipoprotein secretion [6]. Disruption of FA trafficking results in the storage of FA as triglycerides (TG) in the liver, which is one of the consequences of chronic hepatitis [7, 8]. Both HBV and HCV can reprogram the host FA metabolism [7–9]. HCV utilizes β -lipoproteins such as very low density lipoprotein (VLDL) and low density lipoprotein (LDL) to coat itself and hide from the host immune system. HCV uses the LDL receptor (LDLR) for entry into the hepatocytes [10]. Recent studies have discovered that covalently closed circular DNA (cccDNA) of HBV not only attributes to the continuous intrahepatic pool of HBV, the expression of large excess of small surface antigen and its presence in the circulation within non-infectious lipid vesicles contribute to the chronic immune dysfunction in CHB patients [11].

The role of 18–22 nucleotide long microRNAs (miRNAs) in the maintenance of TG homeostasis under pathological condition has been documented [12]. Upon HCV infection, several miRNAs involved in FA synthesis, oxidation and secretion are dysregulated [12, 13], but miRNAs manipulating both lipid metabolism and viral replication are limited. MiR-27a has been reported to be suppressed in Huh7 cells infected with HCV, while it has been shown to repress the major transcription factor, RXR- α and lipid transporter ABCA1 [14] along with multiple genes from lipid metabolism pathways such as FASN, SREBP1, SREBP2, PPAR α , and PPAR γ , ApoA1, ApoB100, and ApoE3, which are required for infectious HCV particle production. MiR-27b has been shown to

restrict cholesterol biosynthesis in Huh7 cells by blocking HMG-CoA reductase, which reduces hepatic TG deposition and HCV copy number [15]. Recently, we reported that miR-c12 could impede FA accumulation and HCV replication by targeting CEP350 and inducing PPAR α mediated transcription of FA β -oxidation genes [16].

In this study, we have shown that the expression of miR-451a dropped significantly in CHC, resulting in the upregulation of its target gene Glycerol Kinase (GK) of lipid metabolism pathway, following which cleaved lipogenic transcription factor SREBP1 became enriched, leading to the accumulation of excess FA, TG, and cholesterol in the liver. Thus, restoration of miR-451a expression inhibited lipid deposition in the liver, exhibited its potential as an antagonist of lipotoxicity and restricted HCV replication as well.

Materials and methods

Details of the study subjects

This study was conducted with archived liver tissue samples and blood collected from treatment naïve chronic hepatitis patients mono-infected with either HCV (CHC) or HBV (CHB) attending the Hepatology clinic of School of Digestive and Liver Diseases, (IPGME&R), Kolkata, India and Indraprastha Apollo Hospital, New Delhi, India. Patients co-infected with HAV/HDV/HEV/HIV, having co-morbidities like chronic alcoholism, diabetes mellitus, autoimmune diseases and unwilling to enrol in the study were excluded. Patients were categorized as CHB or CHC, LC and HCC after detailed assessment of clinical, biochemical, virological and histological evidences. Both CHC and CHB patients ($n=21$, $n_{\text{HCV/CHC}}=7$, $n_{\text{HBV/CHB}}=14$) were having high viral load, ALT > 40IU/L and with active necro-inflammation. Seventeen patients diagnosed with esophageal or gastric varices, portal hypertension, splenomegaly, ascites etc. were included as decompensated LC ($n=17$, $n_{\text{HCV/LC}}=7$, $n_{\text{HBV/LC}}=10$). HCC patients ($n=21$, $n_{\text{HCV/HCC}}=12$, $n_{\text{HBV/HCC}}=9$) were confirmed with triphasic CT scan and/or AFP value (> 250ng/ml).

Normal liver biopsy tissue was collected from Gall bladder carcinoma patients ($n=11$) during cholecystectomy at Department of Gastro-Intestinal Surgery, IPGME&R as routine evaluation of liver metastasis and confirmed after assessment of histological, clinical and biochemical records. Details of patient is presented in Supplementary Table 1.

Sample collection

Percutaneous biopsy and explanted liver tissues were collected in RNA later (Merck, #R0901) and 10% formalin immediately after biopsy or surgery. The tubes with RNA later were kept for 24 h at 4 °C for proper penetration of RNA later in the tissue and then preserved at -80 °C. Formalin tubes were stored at room temperature for future use.

Total RNA isolation and cDNA preparation

Total RNA was isolated from tissue and cell line using TRIzol reagent (Thermo scientific) following manufacturer's protocol. The isolated RNA was quantified using Nanodrop (Thermo scientific). About 500ng/2.5 µg total RNA was used for cDNA synthesis of miRNA/mRNA using miScript PCR Starter Kit (Qiagen, catalog#218193).

Quantitative reverse transcriptase PCR (qRT-PCR)

cDNA was quantified using PowerUpTMSYBR Green PCR master mix (Thermo scientific) and gene specific primers in the QuantStudio 7 Flex RT-PCR machine (Thermo scientific). miR-103a-3p and 18s rRNA were used as an internal control for miRNA and mRNA respectively. $\text{Log}_2 2^{-(\text{Ct-gene}-\text{Ct-control})} \times 10^3$ was used as a fold change in expression of genes.

Target prediction and pathway analysis

Targets of the miRNA were retrieved using 2 Bioinformatics tools namely TargetScan (www.targetscan.org) and miRWalk (<http://mirwalk.umm.uni-heidelberg.de>). Targets showing total context score ≥ 0.3 were considered for validation. In search of the common targets between these two bioinformatic tools, a Venn diagram was generated using Venny 2.1 (<https://bioinfogp.cnb.csic.es/tools/venny/>). Predicted 28 common targets were subjected to the pathway analysis using DAVID (<https://david.ncifcrf.gov/>), KEGG (<https://www.genome.jp/kegg/pathway.html>) and REACTOME (<https://reactome.org/>). Binding of miRNA to the selected 3'UTR is presented in Supplementary Table 2.

AlphaFold2 machine learning approach was used to determine protein structure and leveraging multi-sequence alignment.

Cell lines and plasmid information

Huh7 and SNU449 cell lines were maintained in Dulbecco's Modified Eagle Medium (DMEM) (Himedia, #AL111) with 10% FBS (GIBCO, #10082139) at 37°C incubator. This cell line was authenticated by short tandem repeat (STR) DNA profiling. Lipofectamine 2000 (Thermo scientific) was used for transfection in both the cell lines.

The plasmid pS52/JFH1 consists of recombinant full-length genome of HCV genotype2a/3 was a kind gift

from Jens Bukh, Copenhagen University Hospital, Denmark [17] and pSVNeo2/HBV, the head to tail dimer was gifted by Prof. Chiaho Shih, University of Texas Medical Branch, Galveston, USA [18] respectively.

Pre-miRNA and 3'UTR sequence of the gene were retrieved from UCSC genome browser (GRCh37/hg19) and the sequence was amplified and cloned in pRNAU6.1^{Neo} vector at BamH1/HindIII sites, and psi-CHECKTM-2 (Promega) vector at Xho1/Not1 sites. The enzyme sites were appended in the primers. pScramble-pre-miRNA was a non-specific premiRNA sequence (pre-miR-c12) cloned in pRNAU6.1^{Neo} vector. MiRNA binding site mutant 3'UTR clone was generated using Site directed mutagenesis (SDM) kit (QuikChange II Site-directed mutagenesis kit, Stratagene, #200521) following manufacturer's protocol. Each primer is listed in Supplementary Table 3.

Every in vitro experiment was performed thrice in duplicate.

3'UTR luciferase assay

Huh7 cells were co-transfected with wild-type GK-3'UTR-Luciferase construct, and vector/pScramble pre-miRNA/pPre-miR-451a/pPre-miR-451a + anti-miR-451a oligo. One set was performed with miR-451a binding site mutated GK-3'UTR-Luciferase construct with pPre-miR-451a. After 48 h of transfection, cells were harvested and subjected to Renilla/Firefly Luciferase assay using Dual Luciferase Reporter assay kit (Promega, #E2920). Luciferase activity was normalized to the vector and scramble pre-miRNA control. Huh7 cells (2×10^4) were seeded on 24-well and transfected with 200ng of wild-type-3'UTR-Luciferase construct alone and with various plasmids/oligonucleotides e.g., pScramble pre-miRNA (300ng), pPre-miR-451a (100ng), pPre-miR-451a (300ng) + scramble anti-miRNA (10-50nM), pPre-miR-451a (300ng) + anti-miR451a oligo (10-50nM). One well was transfected with mutated 3'UTR-luciferase construct (200ng) + pPre-miR-451a (300ng). After 36–48 h luciferase assay was performed using Dual Luciferase Reporter assay kit (Promega, #E2920) in GloMax[®] 20/20 luminometer (Promega). Luciferase activity was normalized to the respective control. miRVana[™] miRNA inhibitor, Negative Control#1 was used as scramble anti-miRNA oligo (ThermoFisher, #4464076).

In vitro HCV RNA transcription

The plasmid S52/JFH1 was linearized by restriction digestion with Xba1 enzyme (NEB) and the 3' single strand overhang was removed with Mung Bean Nuclease (NEB). The linearized plasmid DNA was precipitated with ethanol and then in-vitro transcribed into RNA using MEGAscript T7 Transcription kit following

manufacturer's protocol (Thermo scientific). RNA was purified using Trizol (Thermo scientific).

HCV infection assay

HCV RNA was transfected in 4×10^4 Huh7 cells seeded in a 24 well plate using lipofectamine 2000 (Thermo Scientific). Mock transfected well was used as negative control. After 48 h, conditioned media (CM) containing virus particles (HCVcc) was collected and filtered through 0.45- μ m-pore-size cellulose acetate membrane and preserved at 4°C for future use. To determine the multiplicity of infection (MOI), 1×10^3 Huh7 cells seeded on 96 well plate was infected with serially diluted media and cell proliferation was determined using WST1 reagent (Sigma-Aldrich). MOI at which more than 50% of cells survived was selected for infection assay. Thus, 1×10^4 Huh7 cells were seeded in 24 well plates and transfected with pPre-miR-451a and vector control independently and after 24 h, CM of HCVcc at a dilution of 1:1000 was added. Total RNA was isolated after 72 h and HCV RNA was quantified by X-Tail PCR [19].

Immuno-blot analysis

Total protein was isolated using RIPA buffer, and quantified using Bradford reagent (Merck). About 20–25 μ g of protein was subjected to 16% polyacrylamide gel electrophoresis (PAGE) after boiling at 90°C for 5 min with 2X Laemmli buffer. Gel was transferred to PVDF membrane (GE healthcare, #10600023) and blocked with 5% non-fat milk (MP Biomedical, #902887) 2 h at room temperature. The membrane was probed with a specific primary antibody overnight at 4°C with gentle agitation. Anti-rabbit-horseradish peroxidase-conjugated secondary antibody (SantaCruz) and enhanced chemiluminescence (ECL) kit (Pierce, #SKU 34580) were used to detect specific proteins in ChemiDoc imaging system (Bio-rad).

Co-Immuno-precipitation

Huh7 and SNU449 cells were transfected with required plasmids or oligo and total protein was extracted using RIPA buffer and the extract was incubated with antibody and IgG separately after divided into two tubes. Tubes were incubated at 4°C with gentle agitation. After 16 h, prewashed Protein A/G agarose bead (Sigma) was added and incubated for 1 h. Bead was washed with lysis buffer 3 times and protein was eluted by adding Laemmli buffer, boiled and subjected to PAGE. All antibodies are enlisted in Supplementary Table 4.

Oil red O staining and estimation of intracellular triglyceride (TG) content

Huh7 and SNU449 cells transfected with Vector, pPremiR-451a, and anti-miR-451a separately were fixed with 10% formalin for 30 min. Cells were washed with

PBS and incubated in 60% isopropanol for 5 min. Isopropanol was removed and stained with Oil Red O solution (0.5 gm dissolved in 100% isopropanol and filtered) for 20 min and viewed under light microscope (EVOS XL Core cell imaging system, Life technologies). The intracellular stain was then extracted in isopropanol overnight and quantified in a 96 well plate reader at 492 nm.

TG content in serum samples and intracellular Huh7 cells were quantified using Autozyme Triglyceride colorimetric assay kit following manufacturer's protocol (Accurex Biomedical Pvt. Ltd.). The Huh7 cells were lysed with RIPA buffer followed by incubated with the reagent and the colorimetric reading was taken at 510 nm. The data was normalized with the cellular protein content.

Cholesterol assay

Serum samples were diluted to 1:100 with assay diluent. Diluted cholesterol standards or diluted serum samples (50 μ L) were mixed with freshly prepared reagent (50 μ L) in 96-well microtiter plate, and incubated for 45 min at 37 °C in the dark. Colorimetric reading was measured at 570 nm according to manufacturer's protocol (Cell Biolabs, Inc.). Cellular cholesterol levels were assessed using the Fluorometric Total Cholesterol Assay Kit (Cell Biolabs, # STA-390) following manufacturer's protocol. In brief, cells were washed with cold PBS and treated with 200 μ L of a solution composed of chloroform, isopropanol (7:11) and 0.1% NP-40 for 30 min. The resulting extract was vortexed, and centrifuged at 15,000 g for 10 min. The organic phase was collected, dried and the lipid pellet was reconstituted in 1X assay diluent, and quantified.

Statistical analysis

Statistical analysis was performed in excel or in the Graphpad prism version 7. All the data were presented as mean \pm standard deviation. Unpaired two-tailed Student's t-test or Mann-Whitney test was done for the data with Gaussian and Skewed distribution respectively. p-value<0.05 was considered as statistically significant.

Results

Expression pattern of miR-451a in liver tissue with progressive diseases from normal liver to HCC through chronic hepatitis and LC

The miRNA miR-451a was one of the most downregulated miRNAs in HCV infected HCC liver tissue specimens compared to controls as observed in our next generation sequencing data [GSE140370] [16, 20]. Here, we validated the data using liver tissue samples from progressive disease stages, including CHC, LC, and HCC, and compared with normal by qRT-PCR. We observed that the expression of miR-451a was significantly downregulated with disease progression (Fig. 1A). A significant reduction in expression of miR-451a was also observed

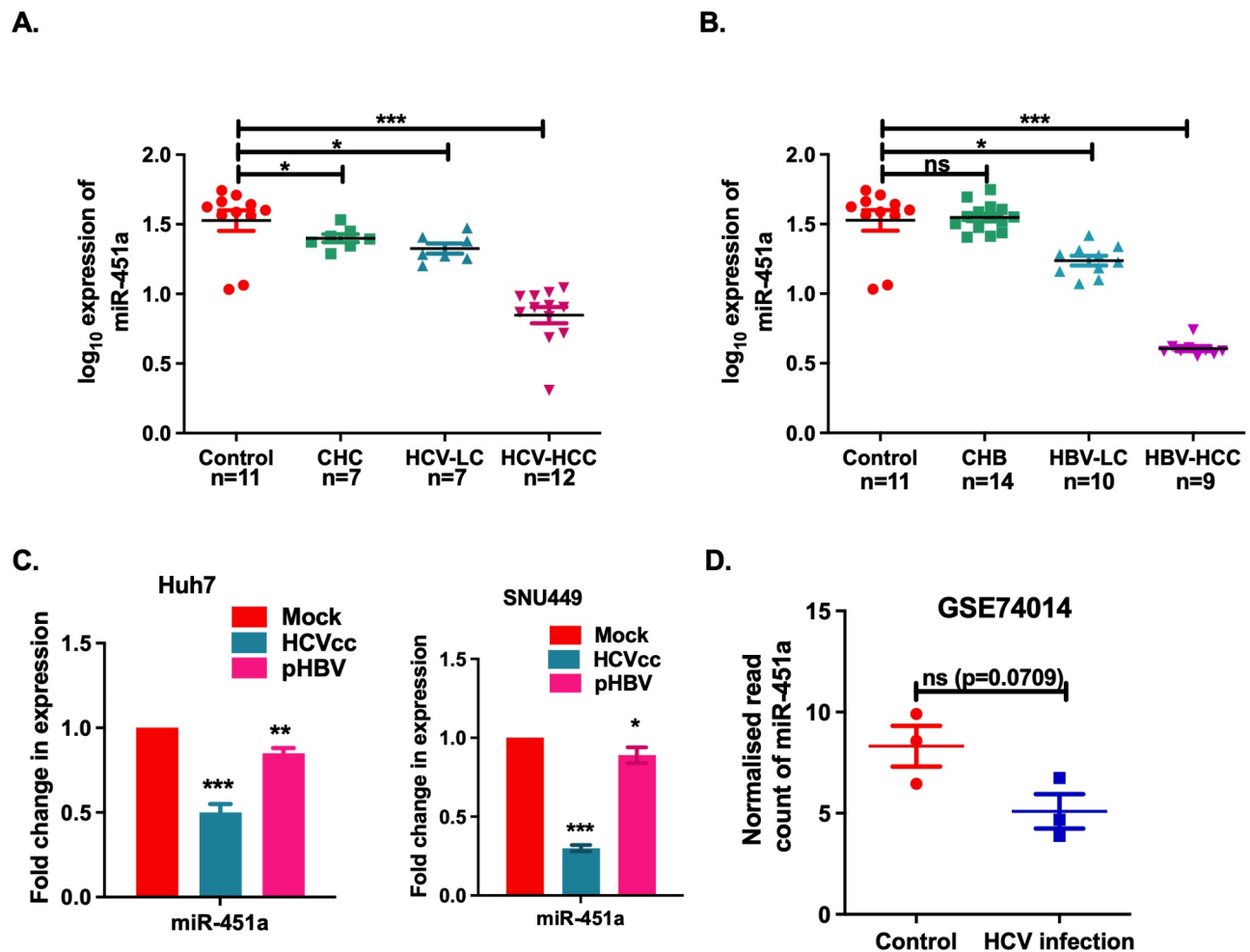


Fig. 1 miR-451a is downregulated in liver tissue of HCV and HBV infected patients. qRT-PCR analysis for the expression of miR-451a (A) and (B) in the liver tissue specimens of progressive liver disease stages of HCV and HBV infection including chronic hepatitis C (CHC)/ chronic hepatitis B (CHB), liver cirrhosis (LC) and hepatocellular carcinoma (HCC) along with normal liver, (C) Huh7 & SNU449 cells were either infected with HCVcc (HCV cell culture) or transfected with HBV producing plasmids pSV2neoHBV2x (pHBV) and compared with mock. (D) miR-451a expression was validated using GSE74014 (HCV infected Huh7.5.1 cells vs. Control). p value was calculated using Mann-Whitney test for (A), (B), and (D). Unpaired student's t test was used for (C). *, **, *** indicate p value < 0.05, < 0.01, and < 0.001 respectively. ns means not significant

from CHB to HBV-LC and HBV-HCC, but no significant alteration was noted between normal and CHB (Fig. 1B). The data were also validated in Huh7 and SNU449 cell lines, either infected with sub-genomic replicon of HCV (HCVcc) or transfected with a plasmid carrying full-length genome of HBV for 48h, respectively. A significant downregulation of miR-451a expression was observed in both the cell lines upon viral infection (Fig. 1C), suggesting that miR-451a might have a protective role not only in HCC but also in CHC and CHB. The data were verified in GEO datasets (GSE74014), where we noted that miR-451a was low in HCV-infected Huh7.5.1 cell line compared to uninfected cells (Fig. 1D).

As we observed higher significant suppression of miR-451a expression in CHC vs. normal than CHB vs. normal and also in HCC cell lines infected with HCV, we aimed to explore the role of miR-451a in CHC infection.

Identification of targets of miR-451a, pathway analysis and functional validation

To understand the role of miR-451a in the development and progression of CHC, the predicted targets (total context score of >0.3) were identified using two bioinformatics tools such as Targetscan and miRWalk, and 28 common target genes were retrieved as presented in the Venn diagram (Fig. 2A). KEGG pathway analysis with these 28 common target genes revealed that the 'metabolic pathways' was the most enriched pathway, which could be impacted by the downregulation of miR-451a (Fig. 2B). Glycerol kinase (GK) was selected as a major target gene in this pathway. Thus, the expression of GK was verified in the liver tissues with progressive liver disease stages by qRT-PCR and was noted that it progressively enhanced from normal to HCV-HCC through CHC, and HCV-LC (Fig. 2C). While upon HBV

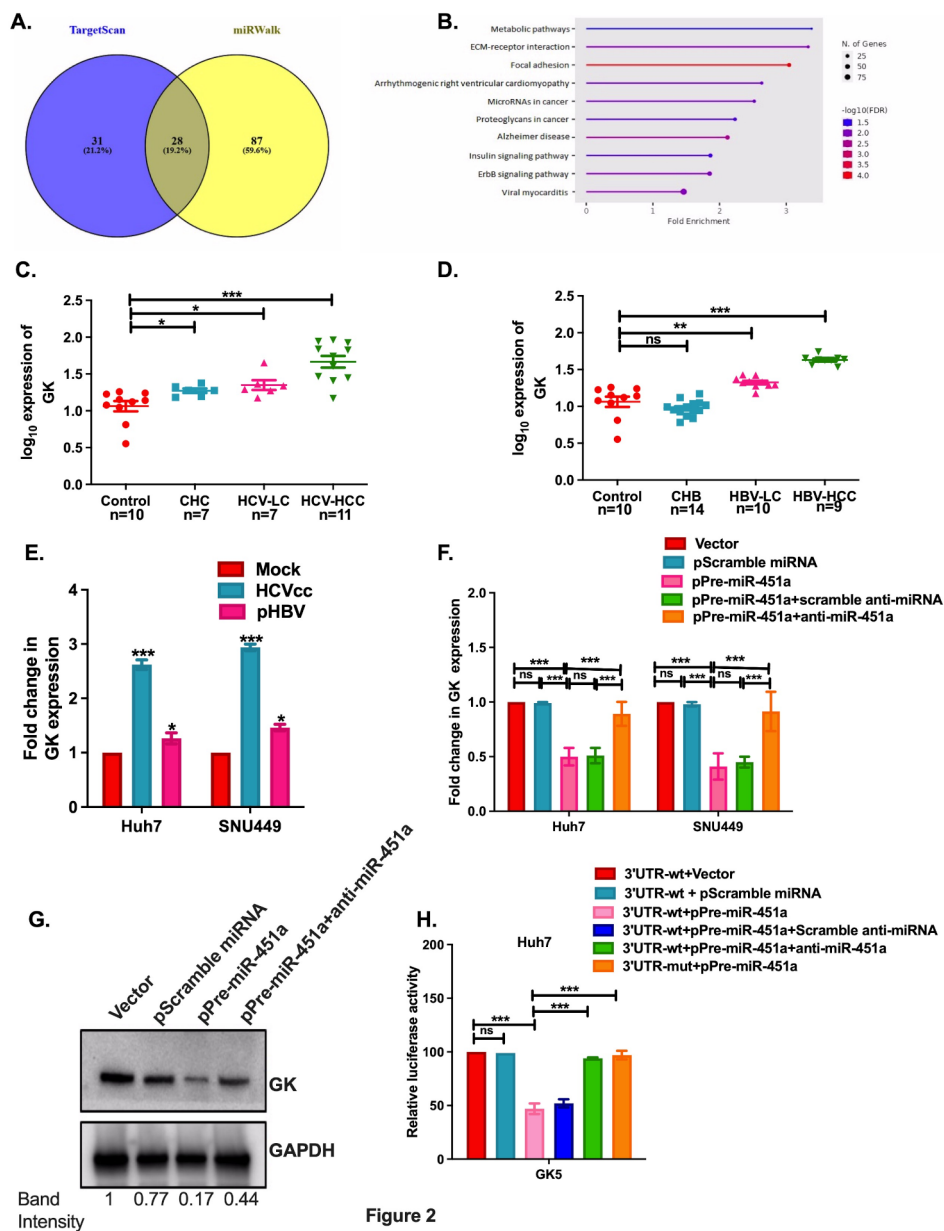


Figure 2

Fig. 2 The miRNA, miR-451a targets metabolic pathway gene glycerol kinase (GK). **(A)** Venn diagram shows 28 common predicted targets retrieved from TargetScan and miRWalk. **(B)** KEGG pathway analysis depicts the significantly altered pathways predicted using 28 direct target genes. qRT-PCR analysis for expression of GK in **(C, D)** liver tissue specimens with progressive liver disease stages of HCV and HBV infection such as CHC/CHB, LC and HCC, **(E)** Huh7 & SNU449 cells either infected with HCVcc (HCV cell culture) or transfected with HBV producing plasmid pSV2neoHBV2x (pHBV) and compared with mock, **(F)** Huh7 and SNU449 cells transfected with empty vector, pScramble-pre-miRNA, pPre-miR-451a, pPre-miR-451a + scramble anti-miRNA, and pPre-miR-451a + anti-miR-451a. **(G)** Immune-blot analysis with anti-GK antibody and anti-GAPDH-HRP using lysates of Huh7 cells transfected with vector, pScramble pre-miRNA, pPre-miR-451a, and pPre-miR-451a + anti-miR-451a. **(H)** 3'UTR-Luciferase reporter assay was performed in Huh7 cells co-transfected with wild-type-3'UTR-Luciferase construct and either vector or pScramble-pre-miRNA or pPre-miR-451a or pPre-miR-451a + scramble anti-miRNA or pPre-miR-451a + anti-miR-451a, and mutated-3'UTR-Luciferase construct + pPre-miR-451a. *p* value was calculated using Mann-Whitney test for **(C, D)**, and unpaired student's *t* test for **(E-G)**. *, and *** indicate *p*-value < 0.05, and < 0.001 respectively. ns means not significant

infection, the expression of GK was amplified in HBV-LC and HBV-HCC compared to CHB but no alteration was seen between normal and CHB (Fig. 2D). A similar significant increase in expression of GK was observed in Huh7 and SNU449 cell lines upon HCV and HBV

infection and the effect was more pronounced with HCV infection (Fig. 2E). Next, Huh7 and SNU449 cells were transfected with pPre-miR-451a and pPre-miR-451a + anti-miRNA-451a and compared with the vector or scrambled miRNA transfected cells. The expression of

GK was decreased in presence of pPre-miR-451a, which reverted back to control level upon anti-miRNA-451a treatment in both qRT-PCR and immune-blot analysis (Fig. 2F and G). To determine the physical association between miR-451a and GK, 3'UTR luciferase assay was performed. A significant decrease in luciferase activity was seen upon co-transfection of GK-3'UTR-luciferase construct and pPre-miR-451a in Huh7 cells compared to vector or pScramble-miRNA treated cells. The luciferase activity was returned to the control level in presence of either anti-miRNA-451a or miR-451a binding site mutant Luciferase construct (Fig. 2H). These data endorsed the binding of miR-451a to the 3'UTR of GK.

GK might regulate intracellular triglyceride content and HCV copy number

To determine the functional impact of GK overexpression on the deregulated metabolic pathways in the liver during chronic progression of liver diseases, we explored the triglyceride (TG) biosynthesis pathway. In this pathway, phosphorylation of glycerol to glycerol-3phosphate by GK is the key rate limiting step that makes the main building blocks for TG. In this context, the expression of FA biosynthesis pathway genes (ACACA, FASN and SCD1) were verified and found to increase with progressive disease stages of HCV infection i.e., CHC to LC and HCC (Figure S1 A-S1C). In vitro HCV infection in Huh7 and SNU449 cells also showed similar higher expression of ACACA, FASN and SCD1, while restoration of miR-451a reduced their expressions (Figure S1D-S1F).

Thus, the intracellular TG, FA, and cholesterol contents were quantified in Huh7 and SNU449 cell lines treated with 50nM of scrambled oligo and GK-anti-sense oligo (ASO). The GK expression level was significantly reduced in both Huh7 and SNU449 cells upon ASO treatment as measured by qRT-PCR and immune-blot analysis (Fig. 3A and B). Intracellular TG content and expression of FA biosynthesis pathway genes (SCD1, ACACA and FASN) were also significantly decreased in both Huh7 and SNU449 cell lines treated with GK-ASO compared to those treated with scrambled oligo, as quantified after Oil Red O staining (Fig. 3C and D) and qRT-PCR, respectively (Fig. 3E and F). Similarly, a reduced level of TG content in Huh7 and SNU449 cells was seen upon restoration of miR-451a and the level was reverted back to normal when cells were treated with anti-miRNA-451a (Fig. 3G and H). Intracellular cholesterol level corroborated well with the above findings. It was lowered in Huh7 and SNU449 cell lines treated with GK-ASO and pPremiR-451a while anti-miRNA-451a treatment restored high intracellular cholesterol level (Fig. 3I and J).

Serum TG and cholesterol levels were examined in the HCV/HBV infected patients across the progressive liver disease stages. While no significant variation was noted

in TG level, serum cholesterol level was significantly dropped with the advancement of the liver disease stages in both CHC and CHB patients (Fig. 4A-D). Intracellular TG and cholesterol levels were determined in Huh7 and SNU449 cells after either infection with HCVcc or transfection with pSVNeo2/HBV. Interestingly, a significant enrichment of both TG and cholesterol was noticed in presence of HCV only (Fig. 4E-H). Upon treatment of Huh7 and SNU449 cells with miR-451a, the increased intracellular TG and cholesterol level in presence of HCV was diminished (Fig. 4I and J). As HCV utilizes VLDL and LDL to form lipo-viral particles to evade host immune response, the intracellular HCV copies (HCVcc) were also measured by qRT-PCR and the data suggested that the HCV copy number was significantly dropped in both HCVcc infected Huh7 and SNU449 cells treated with either miR-451a or GK-ASO compared to control but it was restored back in presence of anti-miR-451a (Fig. 4K-M). So, these data suggests that HCV infection in the hepatocytes suppresses expression of miR-451a which triggers expression of GK and accumulation of TG and cholesterol intracellularly and it is used by HCV for its replication within hepatocytes.

GK might associate with SREBP1 and modifies the lipid metabolism

As SREBPs play a crucial role in the de novo synthesis of FAs, triglycerides and cholesterol and SREBP1 has a positive correlation with GK in different diseases [21–24], the status of SREBP1 was verified in progressive liver disease stages of HCV infection by qRT-PCR. A steady increase in the expression of SREBP1 was observed with the progression of the disease from normal to CHC and also in CHC to LC and HCC (Fig. 5A). qRT-PCR and immune-blot analysis revealed upregulation of SREBP1 upon HCV infection in Huh7 and SNU449 cell lines, particularly the processed active form of SREBP1 while GK-ASO treatment suppressed expression of SREBP1 indicating a mutual regulation between GK and SREBP1 either directly or indirectly (Fig. 5B and C). Further, to investigate the correlation between GK and SREBP1, the SREBP1 was knocked down by treating both Huh7 and SNU449 cell lines with SREBP1-ASO and observed SREBP1 was significantly decreased by qRT-PCR and immune-blot analysis (Fig. 5D). In consistent with the previous data, SREBP1-ASO treated Huh7 and SNU449 cells exhibited lesser TG and cholesterol content than scramble oligo treated cells (Fig. 5E-G) and HCV copy number was also noted relatively less in presence of SREBP1-ASO (Fig. 5H). Next, AlphaFold2 prediction tool was used to determine a possible interaction between GK and SREBP1 in presence of HCV in the liver and observed that these two proteins possibly interacted at 697R-365Y, 625R-489P, 618Q-490Q and 885Y-492 N

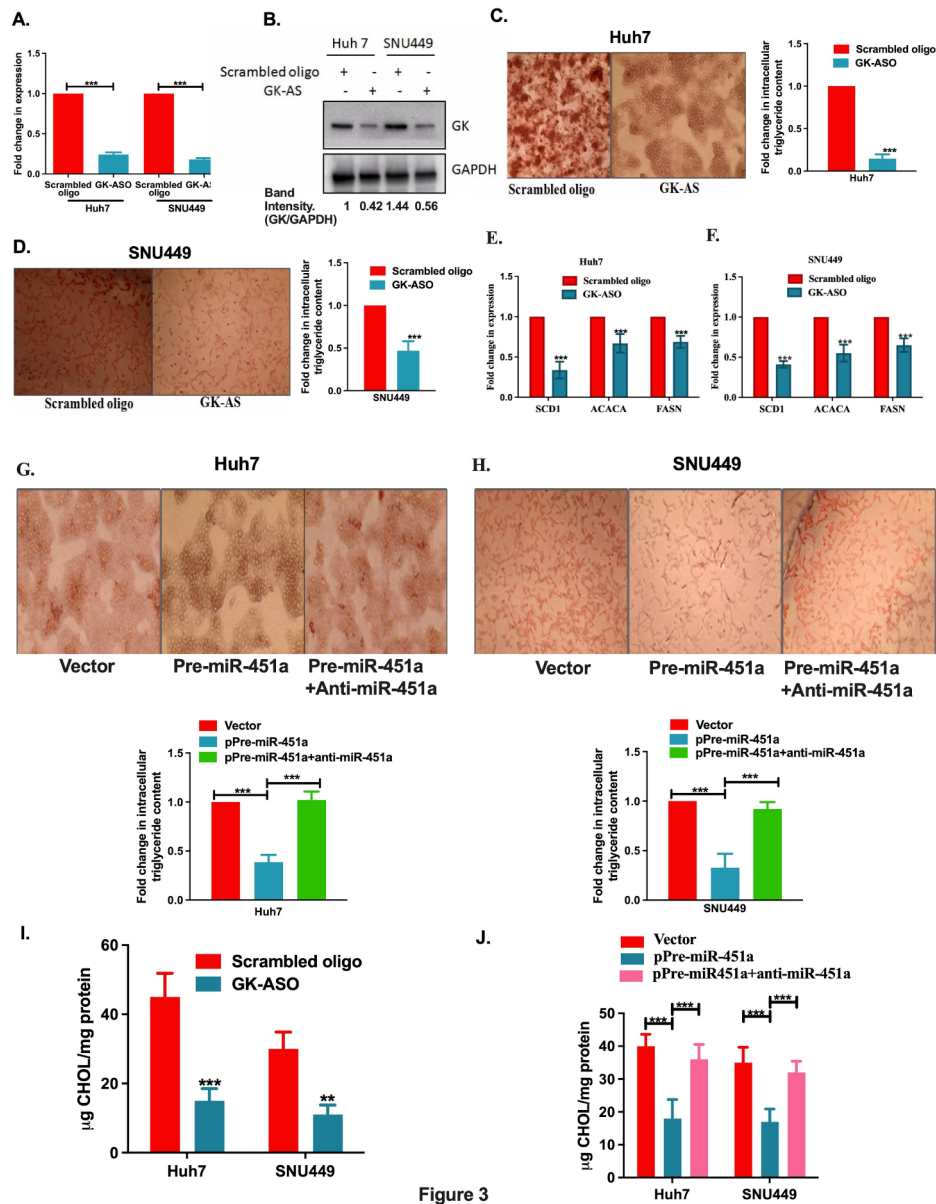


Figure 3

Fig. 3 Role of GK in maintenance of intracellular lipid content and HCV copy number. Both Huh7 and SNU449 cells were treated with 50nM of either scrambled oligo or anti-sense oligo (ASO) specific for GK and the expression of GK was verified by (A) qRT-PCR and (B) Immune-blot analysis with anti-GK antibody. Huh7 and SNU449 cells were treated with GK-ASO and (C) & (D) Oil Red O staining was performed to measure the intracellular triglyceride content, (E) & (F) qRT-PCR analysis was performed to determine expression of fatty acid synthesis genes and (G) cholesterol content was measured using kit. (H-J) Triglyceride and cholesterol content was also measured in Huh7 and SNU449 cells after pPre-miR-451a and pPre-miR-451a + anti-miRNA-451a treatment. *p* value was calculated using unpaired student's *t* test for (A-J). **, ***, **** indicate *p* value < 0.01, < 0.001, and < 0.0001 respectively. ns means not significant

(Fig. 5I). Physical interaction between GK and SREBP1 was confirmed by immune-precipitation of GK with anti-GK antibody using Huh7 cell extract and immunoblotting with anti-SREBP1. In presence of HCV infection, nuclear translocation of SREBP1 was found more than mock and processed SREBP1 showed better interaction with GK (Fig. 5J).

Thus, the overall data depicts that both HCV/HBV infection reduce the expression of miR-451a which targets GK, one of the important kinases in TG biosynthesis pathway. GK positively regulates SREBP1 transcription factor in the liver, as a result TG, FA bio-synthesis and cholesterol accumulated intracellularly and facilitates HCV replication in the hepatocyte resulting disease progression towards end stage liver diseases.

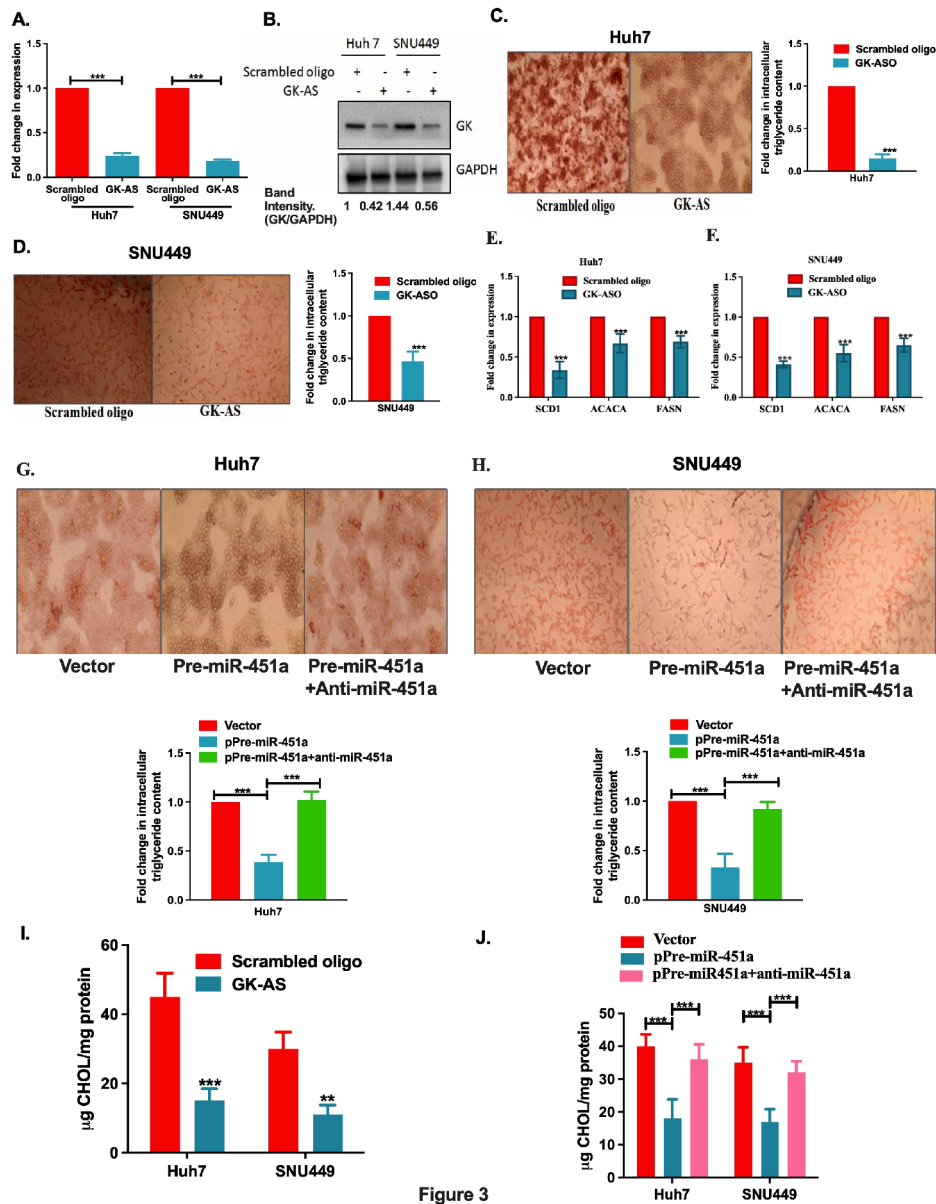


Figure 3

Fig. 4 Glycerol Kinase influences HCV copy number. **(A-D)** Serum triglyceride and cholesterol content was determined in different disease stages of HCV and HBV infection including chronic hepatitis C/B (CHC/CHB), liver cirrhosis (LC) and hepatocellular carcinoma (HCC). **(E-H)** Intracellular triglyceride and cholesterol content was measured in Huh7 and SNU449 cells either infected with HCVcc (HCV cell culture) or transfected with HBV producing plasmid pSV2neoHBV2x (pHBV) and compared with mock. **(I, J)** Intracellular triglyceride, **(K)** cholesterol content determined upon restoration of pPre-miR-451a after HCV-infection in Huh7 and SNU449 cells respectively. Intracellular HCV copy number was measured in both Huh7 and SNU449 cells after treatment with **(L)** pPre-miR-451a **(M)** GK-ASO. p value was calculated using unpaired student's t test for (A-M). *, **, ***, ****; indicate p value < 0.05, < 0.01, < 0.001, and < 0.0001 respectively. ns means not significant

Discussion

In this study, we have characterized a downregulated miRNA, miR-451a in CHC and CHB liver tissue samples in comparison to normal liver suggesting this miRNA might impart a beneficial role to restrict chronic hepatitis. Upon target identification of this miRNA and pathway prediction using bioinformatics tools revealed metabolism was one of the top deregulated pathways in

CHC and GK was the target gene of this miRNA from the lipid metabolism pathway. Though, several miRNAs have been reported to influence lipid metabolism pathways [12–14], miR-451a attributed a dual role in lipid metabolism and in HCV replication as well. GK is one of the rate limiting kinases for TG biosynthesis pathways. Depletion of this kinase was found to be associated with limited biosynthesis of TG, FAs and cholesterol which

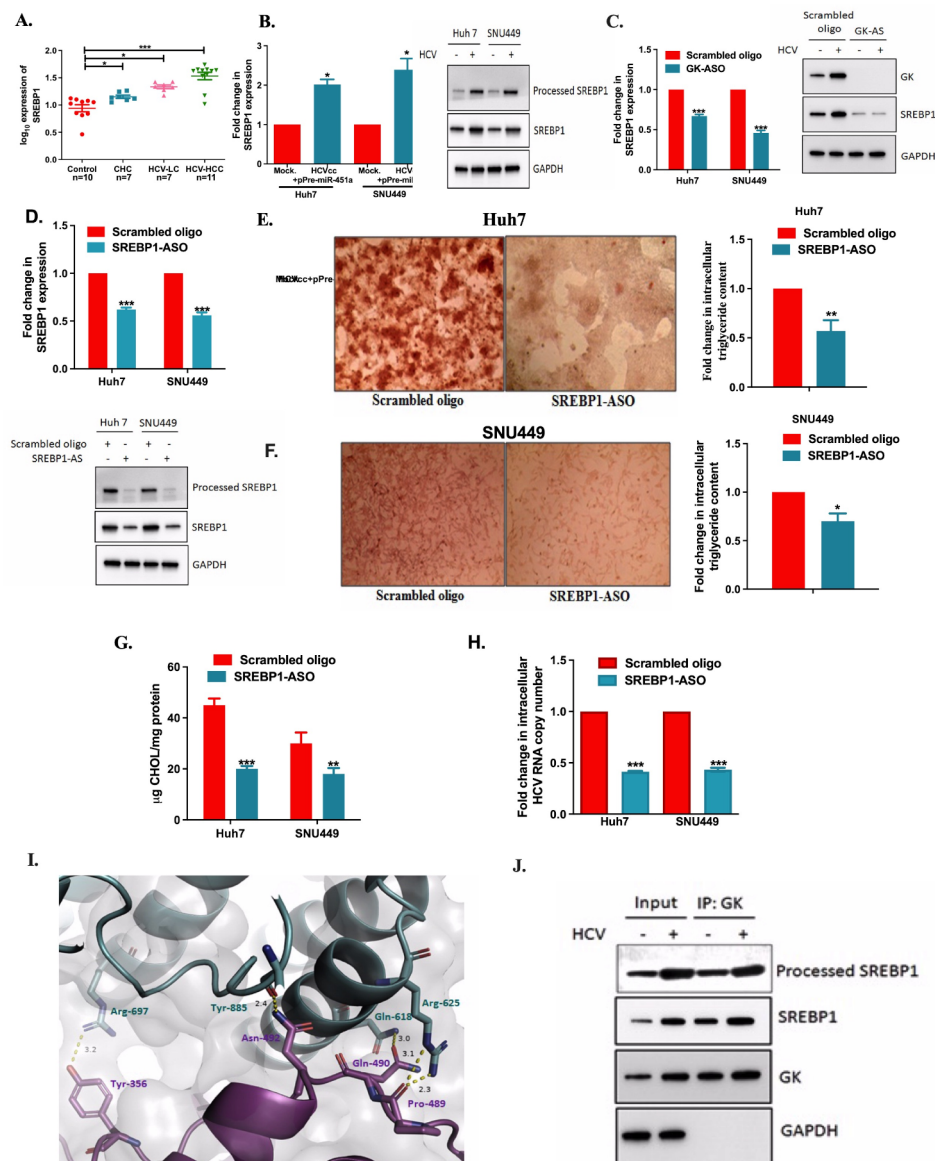


Figure 5

Fig. 5 GK interacts with SREBP1 and the interaction is essential for stabilization. **(A)** SREBP1 expression was verified in **(A)** progressive disease stages of HCV infection that includes chronic hepatitis C (CHC), liver cirrhosis (LC), hepatocellular carcinoma (HCC), **(B)** in Huh7 and SNU449 cell lines infected with HCVcc and **(C)** in Huh7 and SNU449 cell lines treated with GK-ASO (50nM) by qRT-PCR and Immune-blot analysis. **(D)** Expression of SREBP1 was downregulated by SREBP1-ASO (50nM) treatment in Huh7 and SNU449 cells. **(E, F)** Triglyceride and **(G)** cholesterol content was determined in Huh7 and SNU449 cells after SREBP1-ASO treatment. **(H)** HCV copy number was quantified in HCVcc infected Huh7 and SNU449 cells after SREBP1-ASO treatment. **(I)** Interaction between GK and SREBP1 was detected by using Alphafold2 and **(J)** confirmed by immuno-precipitation of HCVcc infected Huh7 cell extract with anti-GK antibody and immunoblotting with anti-SREBP1 antibody in compare with HCV uninfected cells. *p* value was calculated using Mann-Whitney test for **(A)**, and unpaired student's *t* test for **(B-H)**. *, **, *** indicate *p* value < 0.05, < 0.01, and < 0.001 respectively. ns means not significant

restricted replication of HCV in the liver. The transcription factor SREBP1, a central driver of lipogenesis, was also noted to be altered with GK level in the hepatocytes. Thus, our findings illustrated that low level of miR451a in the liver could make individual more sensitive to high fat diet induced hepatic steatosis and fibrosis.

Down regulation of miR-451a has been reported in multiple cancers and a correlation with poor survival

of patients including HCC [25–27]. Kuwabara Y et al., had shown the role of miR-451a in cardiac hypertrophy in type 2 Diabetes Mellitus patients without hypertension through suppression of the LKB1/AMPK pathways [28]. Using NAFLD mice model and patients with NASH it has been found that miR-451a negatively regulated FA induced inflammation via AMPK/AKT pathway [28]. Subsequently, Zheng N et al., had reported the low

expression of miR-451a causing overexpression of its target gene, thyroid hormone responsive spot 14 (THRSP) and high expression of FASN, SCD1 in high fat diet induced NAFLD mice leading to accumulation of TG in the liver [29]. But none of the studies have identified the direct target gene in lipid metabolism pathways. Here, we are showing for the first time the direct impact of suppression of miR451a on lipid metabolism and HCV replication in the hepatocytes. In both CHC/CHB patients miR451a was noted to be downregulated and it intensified the expression of GK. GK phosphorylated glycerol into glycerol 3 phosphate, the building block of TG biosynthesis pathway. GK has been shown to regulate SREBPs (SREBP1a, 1c and SREBP2) which are the transcription factors for genes involved in the biogenesis of TG, FAs and cholesterol [21]. Both overexpression and downregulation of SREBP1 has been noted in cancers [22, 30–32], suggesting it might impart dual functions. Loss of SREBP1 signalling exhibited enhanced lipotoxicity in glioma cells [33] while gain of SREBP1 inhibited apoptosis in pancreatic cancer [34]. In HCC, it induced expression of the FA synthesis genes such as FASN, ACACA, SCD1, restricted FA oxidation, and promoted favourable microenvironment for tumor growth [35]. During hepatic steatosis and fibrosis after HCV infection [36, 37], the core protein of HCV positively regulated the expression of SREBP1 and SREBP1 target genes [38]. Bioinformatics and co-immunoprecipitation analysis revealed a direct interaction between GK and SREBP1.

HBV infection has a direct impact on lipid profile [9]. A significant lower levels of serum TG, HDL, VLDL, and cholesterol have been reported in CHB patients than normal individuals [39]. Our cohort also showed a diminishing trend in the serum TG and total cholesterol level with disease progression though no alterations were seen in HBV infected cell lines.

Hepatic steatosis, Dyslipidaemia and Cardiovascular disease are not only common in CHC, increased level of saturated and mono-unsaturated FA in liver and significantly low level of LDL, HDL, and cholesterol in serum have been also reported in CHB patients. This study confirms the role of the downregulated miRNA, miR-451a in lipid metabolism by direct targeting GK, one of the essential kinases for TG biosynthesis pathway. Restoration of miR-451a reduces expression of FA genes by limiting interaction between GK and SREBP1 resulting less TGs and cholesterol accumulation in the liver. Thus, our data depicted that restoration of miR-451a may combat hepatic lipotoxicity and HCV replication as well by restricting accumulation of FAs, TG, and cholesterol in the liver implying supplementation of this miRNA during therapy of CHC patients may be beneficial.

Abbreviations

ABCA1	ATP-binding cassette subfamily A member 1
ACACA	Acetyl-CoA carboxylase Alpha
APO	Apolipoprotein
cccDNA	Covalently closed circular DNA
DAA	Direct acting antiviral
FA	Fatty acid
FASN	Fatty acid synthase
HBsAg	Hepatitis B Surface Antigen
HBV	Hepatitis B virus
HCC	Hepatocellular carcinoma
HCV	Hepatitis C virus
LC	Liver cirrhosis
LDL	Low density lipoprotein
LDLR	Low density lipoprotein receptor
NAFLD	Non-alcoholic fatty liver diseases
NASH	Non-alcoholic steato-hepatitis
PPAR	Peroxisome proliferator activated receptor
RXR α	Retinoid X receptora
SCD1	Stearoyl-CoA desaturase
SREBP	Sterol regulatory binding proteins
TG	Triglycerides
VLDL	Very low density lipoprotein

Supplementary Information

The online version contains supplementary material available at <https://doi.org/10.1186/s12967-025-06286-9>.

Supplementary Material 1

Supplementary Material 2

Acknowledgements

Authors acknowledged Multidisciplinary Research Unit (MRU) of IPGME&R, Kolkata for providing instrument facility as required. S Majumdar was a recipient of senior research fellowship from the University Grant Commission, Government of India.

Author contributions

S Banerjee and S Majumdar conceived the idea. S Majumdar did most of the in silico and in vitro experiments and D Roychowdhury helped in immune-blot and luciferase assays. A. Chowdhury facilitated to get the liver tissue samples and S Datta read the manuscript carefully. S. Banerjee prepared the final manuscript.

Funding

This work was partly supported by Department of Biotechnology, Government of India and Indian Council of Medical Research, Government of India through BT/PR32493/MED/29/1492/2020 and CTU/PM-ABHIM/17/10/34/2023-ECD-II respectively.

Data availability

The data presented in the manuscript for this study may be available upon request to the corresponding author.

Declarations

Ethics approval and consent to participate

The Ethics Committee of the Institute of Postgraduate Medical Education & Research (IPGME&R), Kolkata has approved the study [Approval ID: Inst/IEC/2015/108; dated 07 July 2015]. Patient's specimen was collected following the declaration of Helsinki and Istanbul. Written informed consent was obtained from all the participants or legal guardians. The study was conducted with archived specimens.

Competing interests

All authors disclosed to have no competing interests.

Author details

¹Centre for Liver Research, School of Digestive and Liver Diseases, Institute of Post Graduate Medical Education and Research, Kolkata, West Bengal, India

²Multi-disciplinary Research Unit, Institute of Post Graduate Medical Education and Research, Kolkata, West Bengal, India

³Department of Hepatology, School of Digestive and Liver Diseases, Institute of Post Graduate Medical Education and Research, Kolkata, West Bengal, India

Received: 11 September 2024 / Accepted: 21 February 2025

Published online: 13 March 2025

References

- Russo FP, Zanetto A, Pinto E, Battistella S, Penzo B, Burra P, Farinati F. Hepatocellular carcinoma in chronic viral hepatitis: where do we stand?? *Int J Mol Sci.* 2022;23(1):500.
- Lazarus JV, Picchio CA, Colombo M. Hepatocellular carcinoma prevention in the era of hepatitis C elimination. *Int J Mol Sci.* 2023;24(18):14404.
- Hsu YC, Huang DQ, Nguyen MH. Global burden of hepatitis B virus: current status, missed opportunities and a call for action. *Nat Rev Gastroenterol Hepatol.* 2023;20(8):524–37.
- Strumillo ST, Kartavykh D, de Carvalho FF Jr, Cruz NC, de Souza Teodoro AC, Sobhie Diaz R, Curcio MF. Host-virus interaction and viral evasion. *Cell Biol Int.* 2021;45(6):1124–47.
- Schneider M, Johnson JR, Krogan NJ, Chanda SK. The Virus–Host interactome: knowing the players to understand the game. *Viral Pathogenesis.* 2016;157–67.
- Mashek DG. Hepatic fatty acid trafficking: multiple forks in the road. *Adv Nutr.* 2013;4(6):697–710.
- Ress C, Kaser S. Mechanisms of intrahepatic triglyceride accumulation. *World J Gastroenterol.* 2016;22(4):1664–73.
- Lonardo A, Adinolfi LE, Loria P, Carulli N, Ruggiero G, Day CP. Steatosis and hepatitis C virus: mechanisms and significance for hepatic and extrahepatic disease. *Gastroenterology.* 2004;126(2):586–97.
- Zhang J, Ling N, Lei Y, Peng M, Hu P, Chen M. Multifaceted interaction between hepatitis B virus infection and lipid metabolism in hepatocytes: A potential target of antiviral therapy for chronic hepatitis B. *Front Microbiol.* 2021;12:636897.
- Samreen B, Khaliq S, Ashfaq UA, Khan M, Afzal N, Shahzad MA, Riaz S, Jahan S. Hepatitis C virus entry: role of host and viral factors. *Infect Genet Evol.* 2012;12(8):1699–709.
- Hyrina A, Burdette D, Song Z, Ramirez R, Okesli-Armlovich A, Vijayakumar A, Bates J, Trevaskis JL, Fletcher SP, Lee WA, Holdorf MM. Targeting lipid biosynthesis pathways for hepatitis B virus cure. *PLoS ONE.* 2022;17(8):e0270273.
- Moore KJ, Rayner KJ, Suárez Y, Fernández-Hernando C. The role of MicroRNAs in cholesterol efflux and hepatic lipid metabolism. *Annu Rev Nutr.* 2011;31:49–63.
- Shirasaki T, Honda M, Shimakami T, Horii R, Yamashita T, Sakai Y, Sakai A, Okada H, Watanabe R, Murakami S, Yi M, Lemon SM, Kaneko S. MicroRNA-27a regulates lipid metabolism and inhibits hepatitis C virus replication in human hepatoma cells. *J Virol.* 2013;87(9):5270–86.
- Shaw TA, Singaravelu R, Powdrill MH, Nhan J, Ahmed N, Özcelik D, Pezacki JP. MicroRNA-124 regulates fatty acid and triglyceride homeostasis. *iScience.* 2018;10:149–57.
- Li HC, Yang CH, Lo SY. Roles of MicroRNAs in hepatitis C virus replication and pathogenesis. *Viruses.* 2022;14(8):1776.
- Ghosh S, Chakraborty J, Goswami A, Bhowmik S, Roy S, Ghosh A, Dokania S, Kumari P, Datta S, Chowdhury A, Bhattacharyya SN, Chatterjee R, Banerjee S. A novel MicroRNA boosts hyper- β -oxidation of fatty acids in liver by impeding CEP350-mediated sequestration of PPAR α and thus restricts chronic hepatitis C. *RNA Biol.* 2020;17(9):1352–63.
- Gottwein JM, Scheel TK, Hoegh AM, Lademann JB, Eugen-Olsen J, Lisby G, Bukh J. Robust hepatitis C genotype 3a cell culture releasing adapted intergenotypic 3a/2a (S52/JFH1) viruses. *Gastroenterology.* 2007;133(5):1614–26.
- Shih CH, Li LS, Roychoudhury S. In vitro propagation of human hepatitis B virus in a rat hepatoma cell Line. *August 15, 1989.* 86 (16) 6323–7.
- Drexler JF, Kupfer B, Petersen N, Grotto RM, Rodrigues SM, Grywna K, Panning M, Annan A, Silva GF, Douglas J, Koay ES, Smuts H, Netto EM, Simmonds P, Pardini MI, Roth WK, Drosten C. A novel diagnostic target in the hepatitis C virus genome. *PLoS Med.* 2009;6(2):e31.
- Ghosh S, Bhowmik S, Majumdar S, Goswami A, Chakraborty J, Gupta S, Aggarwal S, Ray S, Chatterjee R, Bhattacharyya S, Dutta M, Datta S, Chowdhury A, Dhali GK, Banerjee S. The exosome encapsulated MicroRNAs as Circulating diagnostic marker for hepatocellular carcinoma with low alpha-fetoprotein. *Int J Cancer.* 2020;147(10):2934–47.
- Horton JD, Goldstein JL, Brown MS. SREBPs: activators of the complete program of cholesterol and fatty acid synthesis in the liver. *J Clin Invest.* 2002;109(9):1125–31.
- Guo D, Bell EH, Mischel P, Chakravarti A. Targeting SREBP-1-driven lipid metabolism to treat cancer. *Curr Pharm Des.* 2014;20(15):2619–26.
- DeBose-Boyd RA, Ye J. SREBPs in lipid metabolism, insulin signaling, and beyond. *Trends Biochem Sci.* 2018;43(5):358–68.
- Xiao M, Xu J, Wang W, et al. Functional significance of cholesterol metabolism in cancer: from threat to treatment. *Exp Mol Med.* 2023;55:1982–95.
- Su Z, Ni L, Yu W, Yu Z, Chen D, Zhang E, Li Y, Wang Y, Li X, Yang S, Gui Y, Lai Y, Ye J. MicroRNA-451a is associated with cell proliferation, migration and apoptosis in renal cell carcinoma. *Mol Med Rep.* 2015;11(3):2248–54.
- Zhao J, Li H, Zhao S, Wang E, Zhu J, Feng D, Zhu Y, Dou W, Fan Q, Hu J, Jia L, Liu L. Epigenetic Silencing of miR-144/451a cluster contributes to HCC progression via paracrine HGF/MIF-mediated TAM remodeling. *Mol Cancer.* 2021;20(1):46.
- Wei GY, Hu M, Zhao L, Guo WS. MiR-451a suppresses cell proliferation, metastasis and EMT via targeting YWHAZ in hepatocellular carcinoma. *Eur Rev Med Pharmacol Sci.* 2019;23(12):5158–67.
- Kuwabara Y, Horie T, Baba O, Watanabe S, Nishiga M, Usami S, Izuhara M, Nakao T, Nishino T, Otsu K, Kita T, Kimura T, Ono K. MicroRNA-451 exacerbates lipotoxicity in cardiac myocytes and high-fat diet-induced cardiac hypertrophy in mice through suppression of the LKB1/AMPK pathway. *Circ Res.* 2015;116(2):279–88. <https://doi.org/10.1161/CIRCRESAHA.116.304707>. Epub 2014 Oct 31.
- Zeng N, Huang R, Li N, Jiang H, Li R, Wang F, Chen W, Xia M, Wang Q. MiR-451a attenuates free fatty acids-mediated hepatocyte steatosis by targeting the thyroid hormone responsive spot 14 gene. *Mol Cell Endocrinol.* 2018;474:260–71.
- Chen J, Ding C, Chen Y, Hu W, Yu C, Peng C, Feng X, Cheng Q, Wu W, Lu Y, Xie H, Zhou L, Wu J, Zheng S. ACSL4 reprograms fatty acid metabolism in hepatocellular carcinoma via c-Myc/SREBP1 pathway. *Cancer Lett.* 2021;502:154–65.
- Jia Y, Yan Q, Zheng Y, Li L, Zhang B, Chang Z, Wang Z, Tang H, Qin Y, Guan XY. Long non-coding RNA NEAT1 mediated RPRD1B stability facilitates fatty acid metabolism and lymph node metastasis via c-Jun/c-Fos/SREBP1 axis in gastric cancer. *J Exp Clin Cancer Res.* 2022;41(1):287.
- Fukuda M, Ogasawara Y, Hayashi H, Okuyama A, Shiono J, Inoue K, Sakashita H. Down-regulation of glutathione peroxidase 4 in oral Cancer inhibits tumor growth through SREBP1 signaling. *Anticancer Res.* 2021;41(4):1785–92.
- Geng F, Zhong Y, Su H, Lefai E, Magaki S, Cloughesy TF, Yong WH, Chakravarti A, Guo D. SREBP-1 upregulates lipophagy to maintain cholesterol homeostasis in brain tumor cells. *Cell Rep.* 2023;42(7):112790.
- Zhou C, Qian W, Li J, Ma J, Chen X, Jiang Z, Cheng L, Duan W, Wang Z, Wu Z, Ma Q, Li X. High glucose microenvironment accelerates tumor growth via SREBP1-autophagy axis in pancreatic cancer. *J Exp Clin Cancer Res.* 2019;38(1):302.
- Su F, Koerberle A. Regulation and targeting of SREBP-1 in hepatocellular carcinoma. *Cancer Metastasis Rev.* 2024;43(2):673–708.
- Schuppan D, Krebs A, Bauer M, Hahn EG. Hepatitis C and liver fibrosis. *Cell Death Differ.* 2003;10(Suppl 1):S59–67.
- McPherson S, Jonsson JR, Barrie HD, O'Rourke P, Clouston AD, Powell EE. Investigation of the role of SREBP-1c in the pathogenesis of HCV-related steatosis. *J Hepatol.* 2008;49(6):1046–54.
- Yu JW, Sun LJ, Liu W, Zhao YH, Kang P, Yan BZ. Hepatitis C virus core protein induces hepatic metabolism disorders through down-regulation of the SIRT1-AMPK signaling pathway. *Int J Infect Dis.* 2013;17(7):e539–45.
- Araim SQ, Talpur FN, Channa NA, Ali MS, Afridi HI. Serum lipid profile as a marker of liver impairment in hepatitis B cirrhosis patients. *Lipids Health Dis.* 2017;16(1):51.

Publisher's note

Springer Nature remains neutral with regard to jurisdictional claims in published maps and institutional affiliations.